CHARACTERIZATION OF NANOPARTICLE LOADING IN AEROSOLS FOR PULMONARY NUCLEIC ACID DELIVERY

by

Nicole Gill

A thesis submitted to the Faculty of the University of Delaware in partial fulfillment of the requirements for the degree of Honors Degree in Chemical Engineering with Distinction

Spring 2024

CHARACTERIZATION OF NANOPARTICLE LOADING IN AEROSOLS FOR PULMONARY NUCLEIC ACID DELIVERY

by

Nicole Gill

Approved: _____
Catherine A. Fromen, Ph.D
Professor in charge of thesis on behalf of the Advisory Committee

Approved: _____
Millicent O. Sullivan, Ph.D
Committee member from the Department of Chemical and Biomolecular Engineering

Approved: _____
Chitraleema Chakraborty, Ph.D
Committee member from the Board of Senior Thesis Readers

Approved: _____
Michael Chajes, Ph.D.
Dean, University Honors Program

ACKNOWLEDGMENTS

I would like to thank the members of the Fromen lab for their continued support and guidance throughout my undergraduate research career. I would also like to thank Dr. Millicent Sullivan and Hugo Hu for their generous guidance, support, and mentorship throughout the thesis process. In particular, I would like to thank and acknowledge Michael Trautmann-Rodriguez for his continuous mentorship throughout my time in the Fromen Lab. From cell culture training and manuscript writing to helping me design experiments and prepare presentations, my experience, completion of my thesis, and growth as a researcher would not have been possible without his patience and willingness to help me succeed. Lastly, I am hugely grateful to Dr. Catherine Fromen for her invaluable guidance and support throughout my undergraduate career. Without her time and belief in me, I would not have gained a fraction of the experience I have had being a student in her lab, and my future would not look the same.

TABLE OF CONTENTS

LIST OF FIGURES vi
ABSTRACT viii

1 INTRODUCTION 1

1.1 Background and Motivation 1
1.2 Research Goal and Scope 2
1.3 Thesis Overview 4

2 MATERIALS AND METHODS 7

2.1 Measuring Aerosol Droplet Size With Laser Diffraction 7

2.1.1 Nebulization and Size Characterization of Aerosol Droplets 8
2.1.2 Aerosol Droplet Calculation 9
2.1.3 Aerosol Size Correlation With Nebulizer Loading Volume 10
2.1.4 Aerosol Size Correlation With Nanoparticle Concentration 10

2.2 Measuring Aerosol Droplet Size With Microscopy 10

2.2.1 Freezing and Imaging of Aerosol Droplets 11
2.2.2 Using ImageJ to Measure Aerosol Droplet Size 11
2.2.3 Aerosol Droplet Size Calculation 12
2.2.4 Aerosol Droplet Size Correlation With Nanoparticle Loading Concentration 13

2.3 Cellular Nanoparticle Delivery 13

2.3.1 PEGDA Nanoparticle Dosing 14

2.3.1.1 PEGDA Nanoparticle Generation and Characterization 14
2.3.1.2 PEGDA Nanoparticle Liquid and Aerosol Dosing 15

2.3.2 Polyplex Nanoparticle Dosing 17

2.3.2.1 Polyplex Generation and Characterization 17
2.3.2.2 Polyplex Liquid and Aerosol Dosing 18

2.4 Plot Generation and Statistical Analysis 19

3 AEROSOL RESULTS AND DISCUSSION 20

3.1 Aerosol Droplet Size With Laser Diffraction 20

3.1.1 Aerosol Size Correlation With Water Loading Volume 20
3.1.2 Aerosol Size Correlation With Nanoparticle Loading Concentration 24

3.2 Aerosol Droplet Size With Microscopy 26

3.2.1 Aerosol Droplet Size Correlation With Nanoparticle Loading Concentration 26

4 CELLULAR DELIVERY RESULTS AND DISCUSSION 29

4.1 PEGDA Nanoparticle Dosing 29

4.1.1 PEGDA Nanoparticle Characterization 29
4.1.2 PEGDA Nanoparticle Flow Cytometry 29

4.2 Polyplex Nanoparticle Dosing 33

4.2.1 Polyplex Characterization 33
4.2.2 Polyplex Cell Transfection Microscopy 34
4.2.3 Polyplex Cell Transfection Flow Cytometry 36

5 CONCLUSIONS AND FUTURE WORK 40

5.1 Conclusions 40

5.1.1 Physical Effects of Nanoparticle Loading on Nebulized Aerosols 40
5.1.2 Nanoparticle Mediated Nucleic Acid Delivery 41

5.2 Future Work 42

5.2.1 Physical Effects of Nanoparticle Loading on Nebulized Aerosols 42
5.2.2 Nanoparticle Mediated Nucleic Acid Delivery 43

5.3 Impact 43

REFERENCES 45

LIST OF FIGURES

Figure 1: Concept schematic of nebulized nanoparticle-loaded vaccine formulation pathway. Image was made using Biorender. 4

Figure 2: Concept schematic showing the method of laser diffraction.[8] 7

Figure 3: Schematic of experimental method used to characterize nebulized aerosols by laser diffraction. Image was made using Biorender. 8

Figure 4: Using Image J to measure the cross-sectional diameter of aerosolized water droplets in micrographs. 12

Figure 5: A vibrating mesh nebulizer was used along with a 3D printed adapter to deliver nanoparticle loaded aerosols to cells in a 24 well plate. 16

Figure 6: Volume fraction of aerosol droplets per aerosol particle diameter using a 100 µL nebulizer loading volume measured on three separate days. All volume fraction measurements are displayed as the average and standard deviation of three technical replicates. 21

Figure 7: Aerosol cumulative volume fractions versus aerosol particle diameter fit to a third polynomial with 95% confidence intervals for nebulizer loading volumes of 100, 250, and 500 µL..... 22

Figure 8: Calculated VMD for 100, 250, and 500 µL nebulizer loading volumes. Each point is displayed as an average and standard deviation of three experimental replicates. The dashed line represents the average VMD of all three loading volumes. 23

Figure 9: Calculated VMD for 0, 10, 100 and 1000 µg/mL nanoparticle loading concentrations. Each point is displayed as an average and standard deviation of two experimental replicates. The dashed line represents the average VMD of nebulized aerosols without nanoparticles using a 250 µL loading volume. 24

Figure 10: Calculated VMD for 0, 10, 100 and 1000 µg/mL nanoparticle loading concentrations using microscopy. Each point is displayed as an average and standard deviation of three experimental replicates. 27

Figure 11: Relative MFI of Cy5 labeled PEGDA nanoparticles uptaken by A549 cells using liquid and aerosol dosing methods. Relative MFI measurements are displayed as the average and standard deviation of three experimental replicates. *p < 0.05, **p < 0.01, ***p < 0.001, ****p < 0.0001, ns = not significant using Tukey's multiple comparisons tests as part of a one-way ANOVA (n = 3). 30

Figure 12: Relative MFI of A549 cells stained with Zombie Yellow after liquid and aerosol dosing of PEGDA nanoparticles. Relative MFI measurements are displayed as the average and standard deviation of three experimental replicates. *p < 0.05, **p < 0.01, ***p < 0.001, ****p < 0.0001, ns = not significant using Tukey's multiple comparisons tests as part of a one-way ANOVA (n = 3). 32

Figure 13: Micrograph of A549 cells 24 hours after aerosol polyplex dosing. 34

Figure 14: Micrographs of A549 cells 48 hours after liquid and aerosol polyplex dosing. 35

Figure 15: Relative MFI of GFP produced by A549 cells 48 hours after liquid and aerosol dosing of polyplexes. Relative MFI measurements are displayed as the average and standard deviation of three experimental replicates. *p < 0.05, **p < 0.01, ***p < 0.001, ****p < 0.0001, ns = not significant using Tukey's multiple comparisons tests as part of a one-way ANOVA (n = 3). 37

Figure 16: Relative MFI of A549 cells stained with Zombie Yellow 48 hours after liquid and aerosol dosing of polyplexes. Relative MFI measurements are displayed as the average and standard deviation of three experimental replicates. *p < 0.05, **p < 0.01, ***p < 0.001, ****p < 0.0001, ns = not significant using Tukey's multiple comparisons tests as part of a one-way ANOVA (n = 3). 38

ABSTRACT

Approximately 544.9 million people globally are diagnosed with chronic respiratory diseases, which has increased 39.8% since 1990.[1] Aerosolized drugs that can yield controlled effects on the pulmonary immune system may afford new opportunities to treat such diseases. In this research, we investigate the role of nanoparticle formulations as respirable drug delivery carriers. We first investigate the physical effects of nanoparticle loading into nebulized aerosols to create respirable aerosols with tunable sizes. Formulations of different concentrations of nanoparticles were aerosolized with an Aeroneb vibrating mesh nebulizer and characterized by laser diffraction. We find that at a critical nanoparticle concentration, the aerosol volumetric median diameter increased upwards of ~150%. Methods of nucleic acid delivery for pulmonary applications were also explored. Polyplexes were dosed to lung epithelial cells using both liquid and aerosol methods, in which cell transfection was induced successfully using both delivery methods. The results presented in this work have the potential to have significant impacts on particulate aerosol delivery systems, as well as nucleic acid delivery applications. Future work includes combining these physical and cellular effects to improve the transport and delivery of bio-active nanoparticles for immune and gene delivery applications.

Chapter 1

INTRODUCTION

1.1 Background and Motivation

Approximately 544.9 million people globally are diagnosed with chronic respiratory diseases, such as asthma, COPD, and tuberculosis; furthermore, this statistic has increased 39.8% since 1990.[1] Many current therapeutics for respiratory diseases are systemic and do not directly target the lungs. Pulmonary drug delivery has the ability to establish high concentrations of drug in the airways and targeted tissues while lowering undesired absorption, thereby reducing drug resistance and unfavorable side effects.[2] Besides their high bioavailability, inhalable therapeutics are an enticing alternative to oral or intravenous drug delivery due to their immediate effects caused by the large surface area of the lungs, minimal degradation, increased solute permeability, ability to self-administer, and better patient adherence.[3] Therefore, pulmonary drug delivery provides a promising area of research for the development of new respiratory disease therapeutics, including inhalable vaccines.

The mucosal environment of the lungs includes a wide variety of antigen presenting cells, such as alveolar macrophages and dendritic cells, which promptly initiate a cascade of immune responses when an antigen enters the body.[4] Inhalable vaccines have demonstrated increased local efficacy, producing amplified mucosal responses that provide protection directly to the site of pathogen exposure. Despite these advantages, pulmonary drug delivery is not the leading choice for most lung diseases, and inhaled vaccines have yet to become clinically prevalent. The complex

lung mucosal microenvironment, coupled with imprecise aerosol dispersion, limited efficacy aerosol devices, and deficient preclinical testing, has limited inhaled therapies to a few small molecule drugs, such as corticosteroids, and no inhaled immunotherapies have progressed beyond preclinical testing.[5] The lack of inhaled immunotherapies can primarily be attributed to challenges regarding transportation of therapeutics across pulmonary biological barriers as well as non-uniform aerosol formulations. Therefore, there is a critical need to develop inhalable vaccines with precise targeting and controllable deposition in order to achieve a desirable and robust immune response in designated regions of the lung. Failure to meet this critical need would result in reduced vaccine efficacy, as well as variable immune responses, which could lead to numerous cost and safety concerns. To overcome these unique challenges, efficient inhaled delivery formulations must be developed that consider micron sized aerosols for effective lung deposition and nano-sized particles for mucosal penetration and transportation to lymphoid tissue to initiate an immune response. Therefore, an advanced understanding of elements that control aerosol deposition and efficient administration is essential for the formulation and delivery of inhaled mRNA vaccines.

1.2 Research Goal and Scope

The goal of this project is to characterize a formulation pathway for the application of a nebulized nanoparticle-loaded aerosol vaccine delivery system that displays potential on the cellular and macroscopic level. To accomplish this objective, the physical effects of nanoparticle loading into nebulized aerosols will be explored, as well as the effect of loading on nanoparticle-mediated nucleic acid delivery.

Specifically, the effect of nanoparticle loading on nebulized aerosol droplet size will be assessed. When a particulate based formulation is nebulized, an aerosol droplet containing nanoparticles is formed, in which the aerosol droplet size directly impacts where the aerosol droplet deposits in the lung, as depicted in **Figure 1** below. Large aerosol particles, droplets greater than 6 μm in diameter, mostly deposit in the mouth, throat, and upper airway, which severely limits the amount of therapeutic that is delivered to the lungs.[6] Similarly, small aerosol particles, droplets less than 1 μm in diameter, will likely be exhaled, which also limits the delivery and efficacy of the therapeutic to the lungs.[7] Therefore, for efficient lung deposition and treatment of the central and lower airways, aerosol particles should have a diameter between 1 and 5 μm.[6, 7]

The effect of loading on nanoparticle-mediated nucleic acid delivery will be assessed through liquid and aerosol dosing methods. As depicted in **Figure 1** below, after deposition of the nanoparticle loaded aerosol, the nanoparticles must undergo lung mucosal transport to reach desired lung cell targets. Once the nanoparticle is delivered to the cell, the nucleic acid it carries must then transfect the cell, as displayed in the last step of **Figure 1** below.

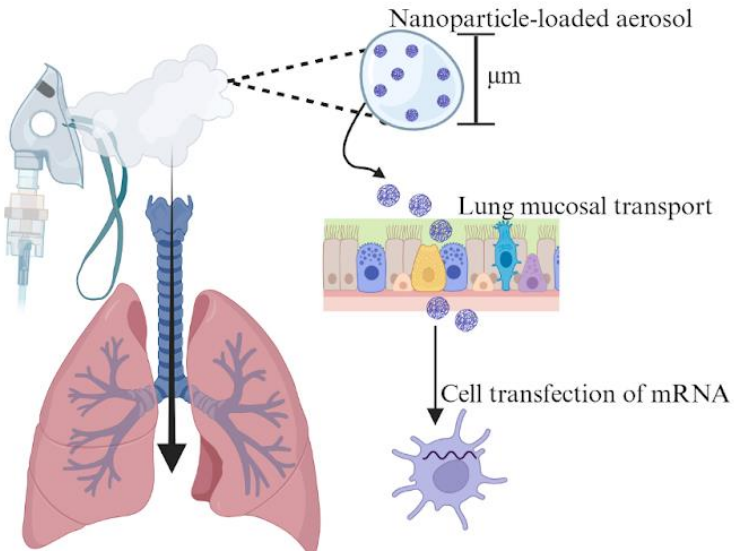

Figure 1: Concept schematic of nebulized nanoparticle-loaded vaccine formulation pathway. Image was made using Biorender.

1.3 Thesis Overview

This thesis is organized into four chapters. In Chapter 2, the materials and methods are described for aerosol characterization using laser diffraction and microscopy, as well as cellular nanoparticle-mediated drug delivery. Within the aerosol characterization methods, there are further subsections for the physical effects of loading volume and nanoparticle concentration on nebulized aerosols. Similarly, the cellular nanoparticle delivery methods are divided into subsections based on particle type. In Chapters 3 and 4, the results of the aerosol characterization and nanoparticle-mediated nucleic acid delivery experiments are analyzed and discussed, respectively. Similar to Chapter 2, the results are divided into subsections depending on aerosol characterization method and particle type. Conclusions and directions for future work are discussed in Chapter 5.

Two specific aims were explored in this thesis and are summarized below. Each of the aims includes their goal, objectives, methods, and key outcomes. The two specific aims of this thesis were to characterize the physical effects of nanoparticle loading into nebulized aerosols and characterize the effect of loading on nanoparticle-mediated nucleic acid delivery.

The first aim that will be explored is the characterization of physical effects of nanoparticle loading into nebulized aerosols. Aerosol size and deposition are major limiting steps of delivering therapeutics to the most effective regions of the lung. I hypothesize that the mucosal transport efficacy of nanoparticle-loaded aerosols is impacted by the amount of nanoparticles loaded within the aerosol, which can be distinguished from aerosol size and altered to increase deposition and mucosal penetration. Starting with model nanoparticles exemplary of potential mRNA nanoparticle carriers, the nebulizer formulation, such as nanoparticle size, charge, and concentration, will be varied in order to create aerosols with tunable nanoparticle loadings and aerosol sizes. The following target ranges of formulation design specifications will be investigated:

1. Aerosols with aerodynamic diameters ranging from 0.3 to 10 microns
2. Nanoparticles with diameters ranging from 200 nm to 1 micron
3. Aerosol nanoparticle loading concentrations ranging from 10 µg/mL to 1 mg/mL

Model mRNA nebulizer solutions will be formulated and aerosolized with an Aeroneb vibrating mesh nebulizer. The resulting aerosol particle size will be characterized by laser diffraction using an optical particle sizer (OPS). I will use a design of experiments approach (DOE) in order to assess the above elements to

optimize formulations of nanoparticle-loaded aerosols for inhaled therapeutics with enhanced mucosal transport.

The second aim that will be explored is the characterization of the effects of loading on nanoparticle-mediated nucleic acid delivery. The lung mucosal environment includes a wid[8]e variety of immune cells, making lung mucosal transport another crucial step to delivering cargo to the right cell types. I hypothesize that the immunogenicity of nanoparticle-loaded aerosols is affected by the dosing method of nucleic acid-loaded nanoparticles. For pulmonary drug delivery applications, nanoparticle-mediated nucleic acid delivery via nebulized aerosols is desired due to the high bioavailability of inhaled therapeutics to the lungs, as well as the other advantages of inhaled delivery discussed previously. Polyplexes will be used to deliver nucleic acids via liquid media and nebulized aerosols to epithelial lung cell line (A549), as described in Hou et al.[6] The effect of liquid versus aerosol dosing of polyplexes on cell transfection will be assessed. Cell transfection efficiency will be determined using flow cytometry and fluorescence microscopy in order to quantify the amount of internalized polyplexes after the cellular delivery of the polyplex loaded liquid and aerosol. By characterizing these effects, optimal dosing strategies for enhanced cell transfection can be developed to increase the immunogenicity of inhaled nucleic acid therapeutics.

Chapter 2

MATERIALS AND METHODS

2.1 Measuring Aerosol Droplet Size With Laser Diffraction

For this thesis, an optical particle sizer (OPS) was used to size aerosol droplets generated with a vibrating mesh nebulizer. The OPS uses laser diffraction to measure aerosol size by directing a laser light beam onto a flow stream of aerosol droplets, causing the aerosol particles in the delivered stream to simultaneously scatter the light.[8] This scattering pattern is then detected and converted to a digital signal that is simplified to an aerosol size distribution in terms of particle volume, calculated using the light intensity and angle relationship of the measured aerosol light scattering pattern.[8] A schematic of the laser diffraction process is displayed in **Figure 2** below.

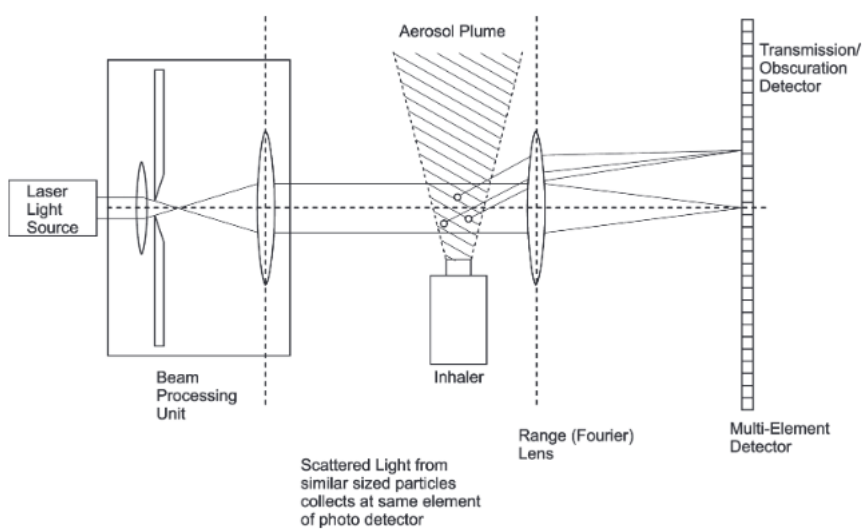

Figure 2: Concept schematic showing the method of laser diffraction.[8]

The measured aerosol droplets are characterized into volumetric diameter size bins, set by the user, in which the final output displayed by the instrument is the number of aerosol droplets in each diameter size bin. The OPS 3330, by TSI, and vibrating mesh nebulizer with a volumetric median diameter (VMD) of four to six microns, by Aerogen, were used. The experimental details and varied nanoparticle conditions are described in the following subsections.

2.1.1 Nebulization and Size Characterization of Aerosol Droplets

To characterize the physical effects of nanoparticle loading on nebulized aerosols, first the desired nanoparticle formulations were made with nanoparticles and water. Next, a constant loading volume of the nanoparticle formulation was loaded into the top of the vibrating mesh nebulizer. A tube about 6 inches in length was used to direct the aerosol generated from the bottom of the vibrating mesh nebulizer into the aerosol collection port of the OPS. **Figure 3** below displays a schematic of the described experimental methods.

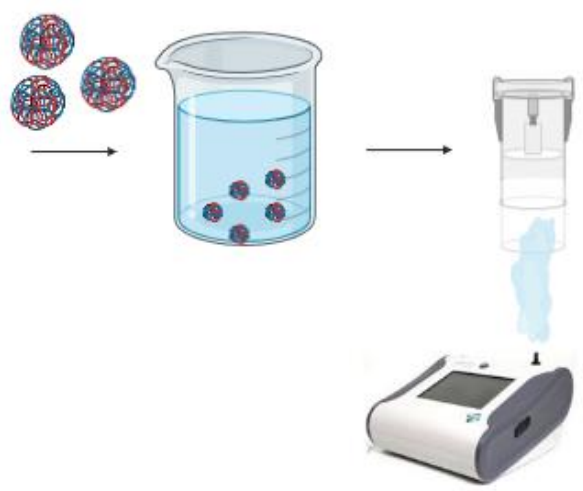

Figure 3: Schematic of experimental method used to characterize nebulized aerosols by laser diffraction. Image was made using Biorender.

The OPS was used to collect aerosols generated from the nebulizer in 30 second durations and characterized the aerosol droplets using laser diffraction into 12 particle diameter size bins: 0.3-0.5, 0.5-0.7, 0.7-1.0, 1.0-1.5, 1.5-2.0, 2.0-2.5, 2.5-3.0, 3.0-4.0, 4.0-5.5, 5.5-6.6, 6.6-8.0, and 8.0-10.0 µm. Three technical replicates of 30 second nebulizations were analyzed per experimental condition, and three experimental replicates were conducted on three different days to account for aerosol variability with variant ambient temperature and humidity.

2.1.2 Aerosol Droplet Calculation

The raw data collected by the OPS reports the number of particles counted per particle diameter size bin. In order to calculate the volumetric median diameter (VMD) of the nebulized aerosols, which is the median droplet size in which half of the total volume of delivered aerosol has smaller droplets and half of the total aerosol volume has larger droplets, the number of particles counted per size bin was converted to volume of particles, assuming the aerosol droplets were perfect spheres. Then, since nebulized aerosol delivery has high variability in the total number of aerosol particles nebulized per 30 second interval, the volume of particles per size bin was normalized to the total volume of the aerosol nebulized in that interval and reported as particle volume fraction per particle diameter size bin. The particle volume fractions per particle diameter size bin were averaged among three technical replicates and plotted as a cumulative volume fraction versus particle diameter. These points were then fitted to a third order polynomial in order to model the aerosol cumulative volume fraction as a function of particle diameter. The VMD is the particle diameter in which the aerosol cumulative volume fraction is 0.5.

2.1.3 Aerosol Size Correlation With Nebulizer Loading Volume

To characterize the effect of nebulizer loading volume on the size of the nebulized aerosol, a series of experiments were conducted that measured the VMD of pure aerosolized water with nebulizer loading volumes of 100, 250, and 500 µL. The nebulization, aerosol characterization, and aerosol size calculation methods were conducted as described in sections 2.1.1 and 2.1.2 above.

2.1.4 Aerosol Size Correlation With Nanoparticle Concentration

To characterize the effect of nanoparticle loading concentration on the size of the nebulized aerosol, a series of experiments were conducted that measured the VMD of nebulized aerosols with nanoparticle loading concentrations of 0, 10, 100 and 1000 µg/mL at a constant loading volume of 250 µL. One micrometer polystyrene particles from PolySciences were diluted in water using a serial dilution technique to achieve the desired nanoparticle loading concentrations. The nebulization, aerosol characterization, and aerosol size calculation methods were conducted as described in Sections 2.1.1 and 2.1.2 above.

2.2 Measuring Aerosol Droplet Size With Microscopy

The size of aerosol droplets generated with a vibrating mesh nebulizer was also measured using microscopy. For these experiments, an Aerogen vibrating mesh nebulizer with a VMD of four to six micrometers was used with the Biotek Cytation 5 Cell Imaging Multi-mode Reader. This was attempted on frozen droplets as described in the following.

2.2.1 Freezing and Imaging of Aerosol Droplets

To characterize the physical effects of nanoparticle loading on nebulized aerosols, first a 6-well cell culture treated, polystyrene plate was prechilled in liquid nitrogen for two minutes. Next, the desired nanoparticle formulations were made with nanoparticles and water, and a 250 µL loading volume of the nanoparticle formulation was loaded into the top of the vibrating mesh nebulizer. The aerosol generated from the bottom of the vibrating mesh nebulizer was sprayed on the prechilled polystyrene plate for five seconds. The aerosol droplets were then frozen on the polystyrene plate with liquid nitrogen for one minute. Once the aerosol droplets were frozen, the polystyrene plate with the aerosol droplets was imaged with the Biotek Cytation 5 Imager.

2.2.2 Using ImageJ to Measure Aerosol Droplet Size

In order to measure the aerosol droplet size, Image J was used to measure the diameter of the aerosol droplet cross section visible in the micrographs. This was done using the line tool to measure and draw a line across the aerosol droplets. For each experimental replicate, at least 300 aerosol droplets were measured. The aerosol cross section diameters were recorded and used to calculate the actual diameter of the droplets to find the VMD. An example replicate is displayed in **Figure 4** below.

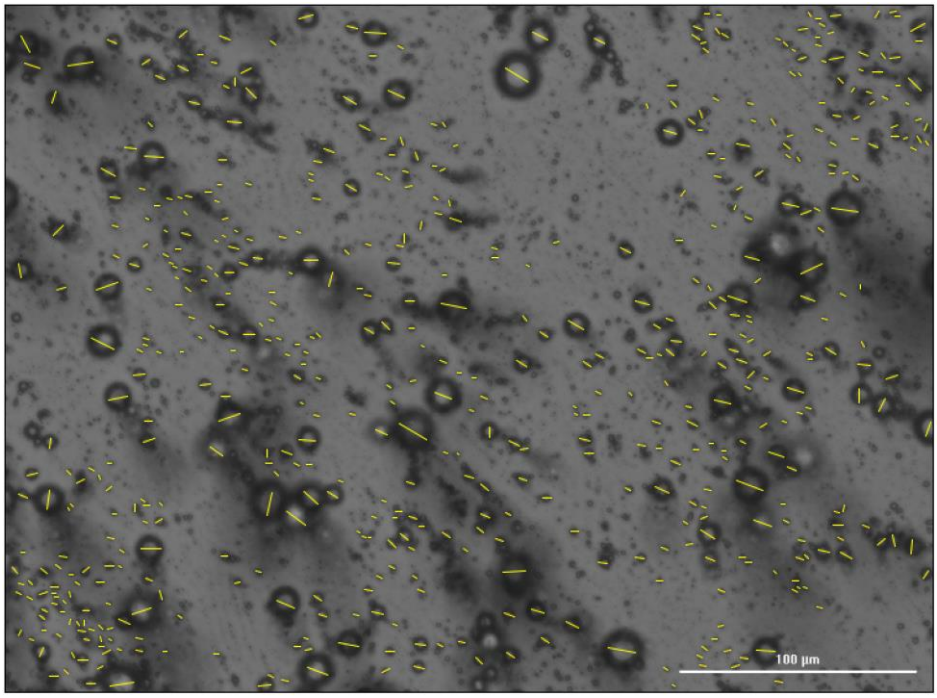

Figure 4: Using Image J to measure the cross-sectional diameter of aerosolized water droplets in micrographs.

2.2.3 Aerosol Droplet Size Calculation

Using the aerosol cross section diameters measured in Image J, the actual diameter of the aerosol particles was calculated in correlation with contact angles. For these experiments, it was assumed that water has a 140° contact angle with cell culture treated polystyrene.[9] With the water contact angle and cross section diameter, the actual radius of the particle was approximated using the formula below.[10] R is the actual radius of the aerosol droplet, R0 is the radius of the aerosol cross section measured from the micrograph, and θ is the contact angle.

$$R = \frac{2^{\frac{2}{3}} R_0}{(1 - \cos\theta)^{\frac{2}{3}} (2 + \cos\theta)^{\frac{1}{3}}}$$

In order to calculate the VMD of the nebulized aerosols, the volume of the aerosol droplets was calculated using the radius of the actual droplet, assuming the aerosol droplets were perfect spheres. Then, since nebulized aerosol delivery has high variability in the total number of aerosol particles nebulized, the volume of particles was normalized to the total volume of the aerosol nebulized onto the polystyrene plate. The aerosol particle volume fractions per particle diameter were averaged among three experimental replicates and plotted as a cumulative volume fraction versus particle diameter. The VMD is the particle diameter in which the aerosol cumulative volume fraction is 0.5.

2.2.4 Aerosol Droplet Size Correlation With Nanoparticle Loading Concentration

To characterize the effect of nanoparticle loading concentration on the size of the nebulized aerosol, a series of experiments were conducted that measured the VMD of nebulized aerosols with nanoparticle loading concentrations of 0, 10, 100 and 1000 µg/mL at a constant loading volume of 250 µL. One micrometer polystyrene particles from PolySciences were diluted in water using a serial dilution technique to achieve the desired nanoparticle loading concentrations. The nebulization, aerosol characterization, and aerosol size calculation methods were conducted as described in Sections 2.2.1, 2.2.2, and 2.2.3 above.

2.3 Cellular Nanoparticle Delivery

To assess the effect of liquid and aerosol dosing on cellular nanoparticle delivery, both poly(ethylene glycol) diacrylate (PEGDA) and polyplex nanoparticles were used. Liquid dosing was performed using traditional cell dosing methods with liquid media loaded with nanoparticles and a pipette. Aerosol dosing was performed

using a vibrating mesh nebulizer to aerosolize both media and PBS loaded with nanoparticles, as described in the following.

2.3.1 PEGDA Nanoparticle Dosing

Before assessing the effects of liquid and aerosol dosing on cell transfection and nucleic acid delivery, control experiments were conducted by dosing inert PEGDA nanoparticles to lung epithelial cells (A549). The following sections describe nanoparticle synthesis, characterization, and dosing methods.

2.3.1.1 PEGDA Nanoparticle Generation and Characterization

PEGDA nanoparticles were synthesized using a reverse emulsion technique as previously described in literature.[11] First, PEGDA (Mn=700) (44.45 wt%), 2- 117 carboxyethyl acrylate (CEA) (2 wt%), photoinitiator diphenyl (2,4,6-trimethylbenzoyl) phosphine oxide (PI) (0.5 wt%), and fluorescent label sulfo-cyanine5 maleimide (Cy5) (0.05 wt%) were dissolved in methanol (MeOH) (50 wt%). Next, 100 μL of the monomer mixture was emulsified in 1 mL of AP1000 silicone oil. The emulsified mixture was then polymerized by irradiation in a UV box for 45 seconds (365 nm at ~28 cm from light source, ~5-10 mW cm-2). Two washes with hexanes and a series of ethanol washes were used to remove unpolymerized monomers and unincorporated Cy5 labels. Following the wash steps, the nanoparticle suspension was passed through a series of sterile 5 μm and 0.45 μm filters to remove micrometer sized particles. The resulting PEGDA nanoparticles were suspended in ethanol and stored at 4 ºC.

In order to determine the concentration of the nanoparticle stock solution, thermogravimetric analysis (TGA) was performed using TA Instruments TGA 550. 50

μL of the nanoparticle solution was loaded onto the TGA sample pans with three technical replicates. The temperature of the samples was ramped to 90 ºC and then held isothermally for 15 minutes to ensure all of the ethanol solvent had evaporated. After the isothermal step, the mass of the nanoparticle solution was measured and the concentration of the nanoparticle stock solution was calculated. After determining the nanoparticle stock solution concentration, dynamic light scattering (DLS) was performed using Malvern Zetasizer Nano S to characterize the hydrodynamic diameter and polydispersity index of the nanoparticles. DLS samples were prepared by diluting the nanoparticle stock solution to 0.1 mg/mL in deionized water.

2.3.1.2 PEGDA Nanoparticle Liquid and Aerosol Dosing

A549 cells were seeded in a 24-well plate with a seeding density of 8*104 cells/well (~4.2*104 cells/cm2) and allowed to adhere for 24 hours. Next, the cells were washed with PBS and dosed with PEGDA nanoparticles. Cells that were administered liquid dosing received 500 μL of media containing nanoparticles at a concentration of 100 μg/mL. Cells that were administered aerosol dosing received 500 μL of PBS containing nanoparticles at a concentration of 1000 μg/mL. The aerosol was generated using a vibrating mesh nebulizer that included a 3D printed adapter between the exit of the nebulizer to the top of the well, as seen in **Figure 5** below. The aerosol dosing concentration used in these experiments was 10 times greater than the liquid dosing concentration since previous experiments in the lab have shown the nebulizer has a yield of approximately 10%, meaning only 10% of the total volume nebulized is delivered to the cells. In order to prevent large proteins from clogging the mesh of the nebulizer, the nanoparticles were suspended in PBS for aerosol delivery, and then 500 μL of media was supplemented on top of the wells. Following the

nanoparticle dosing, the cells were allowed to incubate for 24 hours. After the 24 hour incubation period, the cells were washed twice with PBS to remove unbound nanoparticles. Next, to prepare for cellular viability and nanoparticle uptake analysis, the cells were detached using 0.25% Trypsin-EDTA (Corning), supplemented with 2% FBS, and washed twice with PBS. The cells were then stained with ZombieYellow (Biolegend) at a concentration of 100 μg/mL to test for cell pre-apoptosis. Following staining, the cells were washed twice with PBS and analyzed by flow cytometry using the ACEA NovoCyte Flow Cytometer. Nanoparticle uptake and cell viability were measured by fluorophore median fluorescence intensity (MFI), recorded by the flow cytometer.

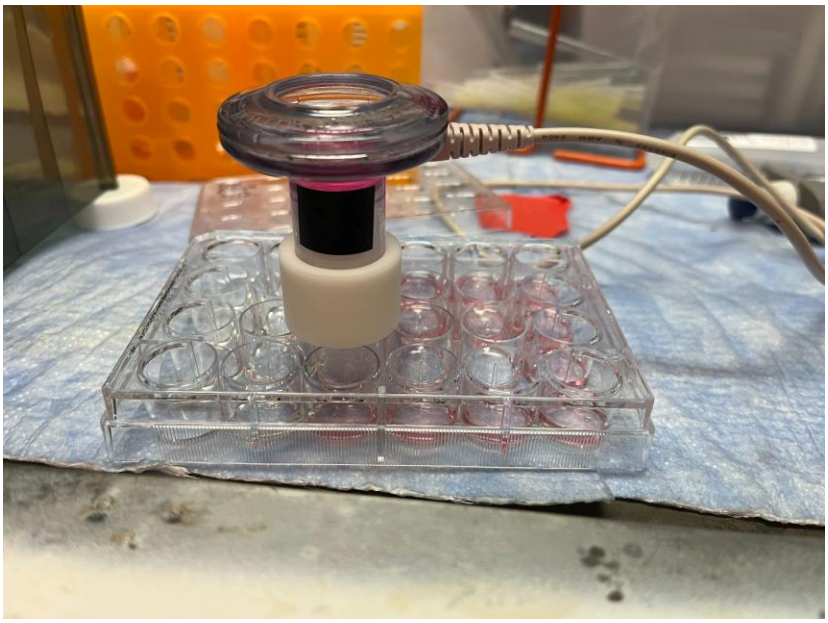

Figure 5: A vibrating mesh nebulizer was used along with a 3D printed adapter to deliver nanoparticle loaded aerosols to cells in a 24 well plate.

2.3.2 Polyplex Nanoparticle Dosing

To evaluate the effects of liquid versus aerosol dosing on cell transfection and nucleic acid delivery, polyplexes loaded with DNA, encoding green fluorescent protein (GFP), were dosed to A549 cells. The following sections describe polyplex synthesis, characterization, and dosing methods.

2.3.2.1 Polyplex Generation and Characterization

Polyplexes were generated with the gWIZ plasmid and a mixture of the cationic polymer poly(ethylenimine) (PEI), following established protocols.[12, 13] In summary, the PEI mixture, as well as a 20 μg/mL pDNA solution, were formulated separately in 20 mM HEPES buffer at a pH of 6. The polycation solution was then added dropwise to an equal volume of pDNA, while gently vortexing, to create polycation-pDNA particles. Following preparation of the polycation-pDNA particles, polyplexes were allowed to form at room temperature for 10 minutes. For these experiments, polyplexes were generated with a N:P ratio of 10, which was calculated as the ratio of the number of amines in the PEI polymer to the number of phosphates in the pDNA.

The size and zeta potential of the polyplexes were determined using DLS on Brookhaven Instruments ZETAPals. All DLS measurements were recorded at a temperature of 25°C with a 658 nm wavelength solid-state laser at an angle of 90°. The hydrodynamic diameter of the particles was determined using 3 sample runs of two minutes each, while the zeta potential was determined using 10 sample runs of 2 minutes each.

2.3.2.2 Polyplex Liquid and Aerosol Dosing

A549 cells were seeded in a 24-well plate with a seeding density of 2*104 cells/well (~1.1*104 cells/cm2) and allowed to adhere for 24 hours. Next, the cells were washed with PBS and dosed with polyplexes. Cells that were administered liquid dosing received 600 µL of incomplete media (media that does not contain FBS) containing polyplexes at a concentration of 20 µg/mL. Cells that were administered aerosol dosing received 800 µL of incomplete media containing polyplexes at a concentration of 20 µg/mL. The aerosol was generated using a vibrating mesh nebulizer without the use of a 3D printed adapter since experiments showed the nebulizer had a yield of approximately 70% without it. Following the polyplex dosing, the cells were allowed to incubate for 2 hours before the media containing the polyplexes was removed and replaced with complete media (media that contains FBS). Next, the cells were allowed to incubate for 48 hours in order for cell transfection to occur. After the first 24 hour incubation period, the cells were imaged using fluorescence microscopy (Zeiss Axio Observer 7) in order to visually assess cell viability and cell transfection by GFP production. After the second 24 hour incubation period, the cells were imaged again using the Biotek Cytation 5 Imager to further visually assess cell viability and cell transfection. Next, to prepare for a quantitative cellular viability and cell transfection analysis, the cells were detached using 0.25% Trypsin-EDTA (Corning), supplemented with 2% FBS, and washed twice with PBS. The cells were then stained with ZombieYellow (Biolegend) at a concentration of 100 µg/mL to test for cell pre-apoptosis. Following staining, the cells were washed twice with PBS and analyzed by flow cytometry using the ACEA NovoCyte Flow Cytometer. Cell transfection and cell viability were measured by fluorophore median fluorescence intensity (MFI), recorded by the flow cytometer.

2.4 Plot Generation and Statistical Analysis

All statistical analysis and plot generation was performed using GraphPad Prism 9 (GraphPad Software Inc.). All quantitative results are reported as the mean and standard deviation of three experimental replicates. Statistical significance was determined using Student's t-test, one way ANOVA, or multiple comparison test, as indicated in figure captions.

Chapter 3

AEROSOL RESULTS AND DISCUSSION

3.1 Aerosol Droplet Size With Laser Diffraction

To characterize the physical effects of nanoparticle loading on nebulized aerosols, the correlation between aerosol droplet size and nanoparticle loading concentration was investigated. This was first done for nanoparticle loading concentrations of 0, 10, 100 and 1000 µg/mL and measured using an OPS, which counted the number of aerosol droplets in specified diameter size bins during a 30 second nebulization period. Before experimentally testing the effects of nanoparticle loading concentration on aerosol droplet size, experimental control experiments were conducted to determine the effect of nebulizer loading volume on aerosol droplet size. The results from these control experiments were used to select a nebulizer loading volume for all subsequent nanoparticle loading concentrations and are outlined in section 3.1.1 below.

3.1.1 Aerosol Size Correlation With Water Loading Volume

Experimental control experiments were conducted to determine the effect of nebulizer loading volume on aerosol droplet size. This was done for nebulizer loading volumes of 100, 250, and 500 µL. For each nebulizer loading volume, three technical replicates were analyzed for three experimental replicates. Each experimental replicate was collected on three separate days to account for aerosol variability with variant ambient temperature and humidity. For each technical replicate, the OPS counted the

number of aerosol droplets in specified diameter size bins during a 30 second nebulization period. Assuming the aerosol droplets were perfect spheres, the number of aerosol droplets per size bin was converted to volume of aerosol droplets and then normalized to the total volume of the aerosol nebulized in that 30 second interval, which are reported as aerosol volume fractions per size bin, as seen in **Figure 6** below.

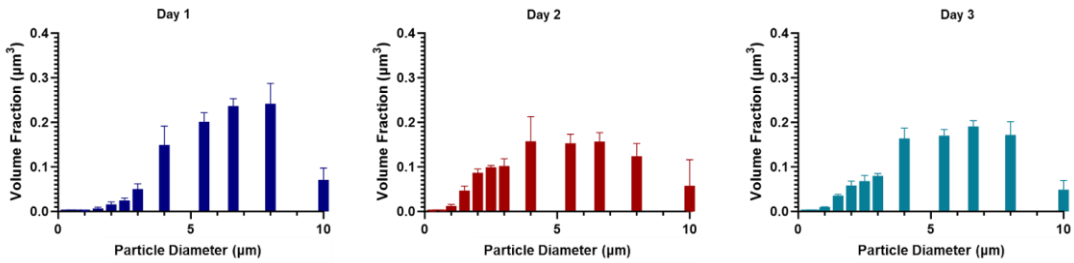

Figure 6: Volume fraction of aerosol droplets per aerosol particle diameter using a 100 µL nebulizer loading volume measured on three separate days. All volume fraction measurements are displayed as the average and standard deviation of three technical replicates.

Figure 6 above displays the volume fraction of aerosol droplets per aerosol particle diameter for a 100 µL nebulizer loading volume on three different days, in which each volume fraction measurement is an average of three technical replicates. Next, the average aerosol volume fractions measured were plotted as cumulative volume fractions versus aerosol particle diameter and fit to a third order polynomial in order to model the aerosol cumulative volume fraction as a function of particle diameter. This experimental analysis was then repeated for 250 and 500 µL nebulizer loading volumes, in which the results are displayed in **Figure 7** below.

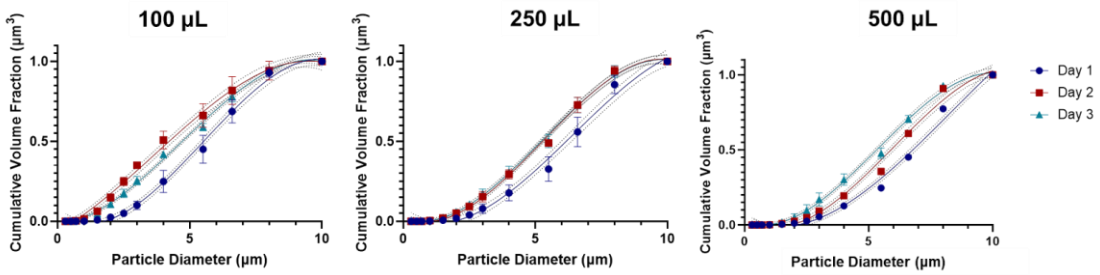

Figure 7: Aerosol cumulative volume fractions versus aerosol particle diameter fit to a third polynomial with 95% confidence intervals for nebulizer loading volumes of 100, 250, and 500 µL.

Figure 7 above displays cumulative volume fractions of the aerosol droplet versus aerosol particle diameter for nebulizer loading volumes of 100, 250, and 500 µL. Each curve is an experimental replicate fit to a third order polynomial function with 95% confidence intervals, in which each point is an average of three technical replicates. A comparison of fits test was conducted to compare the cumulative volume fraction curves across the different days, or experimental replicates, in which it was found that at least one curve was statistically different from the others. This means that there was variability in the aerosol measurements collected on different days, which could be a result of changing ambient temperature and humidity. Using these plots, the VMD of the aerosols for each nebulizer loading volume was determined by finding the particle diameter in which the cumulative volume fraction equals 0.5. The VMD for each experimental replicate of the nebulizer loading volumes was found and plotted in **Figure 8** below.

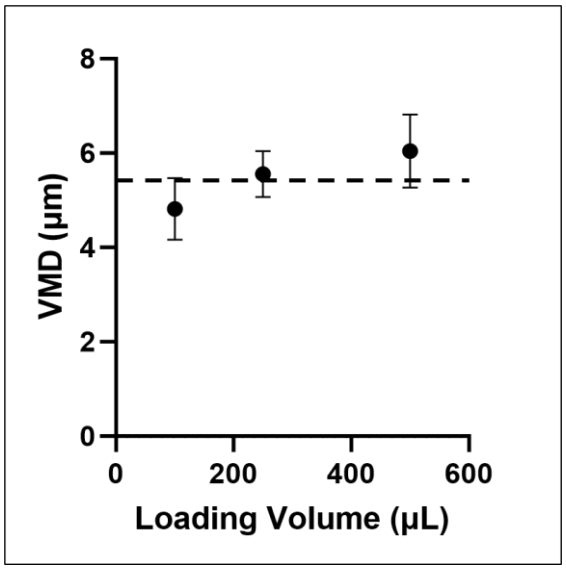

Figure 8: Calculated VMD for 100, 250, and 500 µL nebulizer loading volumes. Each point is displayed as an average and standard deviation of three experimental replicates. The dashed line represents the average VMD of all three loading volumes.

Figure 8 above displays the average VMD of the three experimental replicates for each of the nebulizer loading volumes tested. The average VMD for all loading volumes was also calculated to be 5.5 ± 0.8 µm, which is in agreement with the nebulizer vendor specifications of an expected VMD between 4 µm and 6 µm. A one-way ANOVA was performed on the above data to determine the statistical significance of nebulizer loading volume on aerosol droplet VMD, in which it was found that there is no statistical difference between the calculated VMD for each loading volume. Therefore, nebulizer loading volume has no effect on the size of the nebulized aerosol. With this conclusion, a 250 µL nebulizer loading volume was used for all subsequent experiments.

3.1.2 Aerosol Size Correlation With Nanoparticle Loading Concentration

After concluding that the nebulizer loading volume has no effect on the size of the nebulized aerosol, the effect of nanoparticle loading concentration on the size of the aerosol droplet size was investigated. For these experiments, a constant nebulizer loading volume of 250 µL was used and the following nanoparticle loading concentrations were tested: 0, 10, 100 and 1000 µg/mL. The same experimental methodology and analysis described in section 3.1.1 above to determine the VMD of nebulized aerosols was used for all nanoparticle loading concentration experiments. The results of these experiments are displayed in **Figure 9** below.

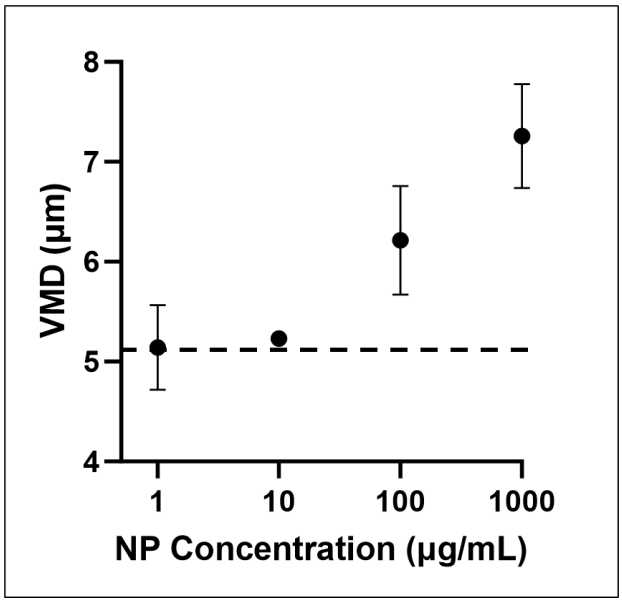

Figure 9: Calculated VMD for 0, 10, 100 and 1000 µg/mL nanoparticle loading concentrations. Each point is displayed as an average and standard deviation of two experimental replicates. The dashed line represents the average VMD of nebulized aerosols without nanoparticles using a 250 µL loading volume.

As seen in **Figure 9** above, the VMD of the nebulized aerosol without nanoparticles was consistent with the VMD of the nebulized aerosols in the loading volume experiments analyzed previously. The VMD of the nebulized aerosols with a 10 µg/mL nanoparticle loading concentration was approximately equivalent to the VMD of the aerosols without nanoparticles. This is to be expected with such a low concentration of relatively large, 1 micron, nanoparticles, since it is likely that not all of the nebulized aerosol droplets contained nanoparticles at this loading concentration. Nanoparticle loading concentrations of 100 and 1000 µg/mL increased the VMD of the nebulized aerosols by 1.1 and 2.1 µm, respectively, which are 21.4% and 40.9% increases in diameter. This preliminary data suggests that the size of nebulized aerosols increases with increasing nanoparticle concentration. However, since only two experimental replicates were completed, a statistical analysis could not be conducted to determine whether this increase in aerosol size was statistically significant.

Due to experimental limitations and challenges, only two replicates were obtained to characterize the effects of nanoparticle loading concentration on the size of nebulized aerosols. This can be attributed to complications with measuring the size of liquid aerosols with the OPS. Since the nanoparticles for these experiments were nebulized in water, when the nebulized aerosol was flown through the machine, the water would condense and accumulate within the machine, which would contaminate the laser box, rendering the instrument unusable. Therefore, the OPS cannot be used as an effective method to measure the size of liquid aerosols.

3.2 Aerosol Droplet Size With Microscopy

As an alternate method to characterize the correlation between aerosol droplet size and nanoparticle loading concentration, microscopy and image analysis methods were used. This was done for nanoparticle loading concentrations of 0, 10, 100 and 1000 µg/mL. Nanoparticle loaded aerosols were nebulized onto a 6 well plate, frozen with liquid nitrogen, and imaged using the Biotek Cytation 5 Imager. Image J was then used to measure the cross-sectional diameter of the droplets, which were converted to the actual aerosol droplet diameter using contact angle calculations. The VMD of the nebulized aerosols was found by calculating and plotting the aerosol cumulative volume fraction versus the aerosol diameter. The results of these experiments are displayed in section 3.2.1 below.

3.2.1 Aerosol Droplet Size Correlation With Nanoparticle Loading Concentration

For each nanoparticle concentration tested, three experimental replicates were conducted, in which the resultant VMD of the nebulized aerosols is displayed as an average and standard deviation in **Figure 10** below.

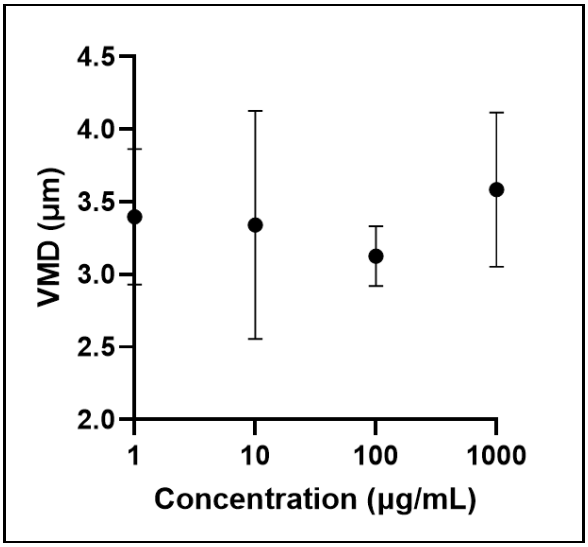

Figure 10: Calculated VMD for 0, 10, 100 and 1000 µg/mL nanoparticle loading concentrations using microscopy. Each point is displayed as an average and standard deviation of three experimental replicates.

As seen in **Figure 10** above, the microscopic method shows no correlation between nanoparticle loading concentration and aerosol VMD. Unlike the laser diffraction results, the VMD of the aerosols measured using microscopy had a similar average with large standard deviations across all nanoparticle concentrations, indicating that the aerosols are the same size regardless of nanoparticle loading concentration. However, these results are likely inaccurate given the limitations of this experimental method. Given that these aerosols were frozen in liquid nitrogen before imaging, the accurate size representation of the aerosols was dependent on the aerosols remaining frozen long enough for the imaging process. Once the frozen aerosols began to melt, the droplets would move and aggregate together, invalidating the results. Furthermore, the microscopic method did not have a high enough resolution to quantify a significant change in aerosol size. From the laser diffraction results, the

largest size increase between 0 and 1000 µg/mL nanoparticle loading concentrations was approximately 2 µm. This change is likely too small to be accurately measured using microscopy and Image J analysis, especially the small, incremental size changes for the intermediate nanoparticle loading concentrations. Additionally, the VMD measured using microscopic methods is approximately 30% smaller than the VMD of the aerosols measured using laser diffraction. This could be due to inaccurate contact angle assumptions since the aerosols were nebulized onto cell culture treated polystyrene rather than uncoated polystyrene. Therefore, the aerosol characterization results using microscopy are inconclusive, and more sensitive measurement techniques, such as laser diffraction, should be used.

Chapter 4

CELLULAR DELIVERY RESULTS AND DISCUSSION

4.1 PEGDA Nanoparticle Dosing

Control experiments using inert PEGDA nanoparticles were conducted to provide a base standard of nanoparticle uptake by A549 cells using both liquid and aerosol dosing methods. These results were also used to isolate the effects of aerosol dosing, as opposed to liquid dosing, such as cell apoptosis.

4.1.1 PEGDA Nanoparticle Characterization

PEGDA nanoparticles were generated and characterized to determine sample concentration, hydrodynamic diameter, and polydispersity index (PDI). The sample was found to have a hydrodynamic diameter of 424.3 nm and a PDI of 0.423. This particle size is consistent with synthesis values reported in literature.[11] However, the measured PDI indicates that the nanoparticles were moderately polydisperse.

4.1.2 PEGDA Nanoparticle Flow Cytometry

In order to characterize the effects of liquid and aerosol dosing on PEGDA nanoparticle uptake by A549 cells, there were four treatment groups: the liquid control group was dosed with complete liquid media without nanoparticles, the liquid PEGDA group was dosed with complete liquid media containing nanoparticles at a concentration of 100 µg/mL, the aerosol control group was dosed with aerosolized PBS without nanoparticles, and the aerosol PEGDA group was dosed with aerosolized

PBS containing nanoparticles at a concentration of 1000 µg/mL. Flow cytometry was used to quantify cellular nanoparticle uptake by measuring Cy5 fluorescence, in which the results are displayed in **Figure 11** below.

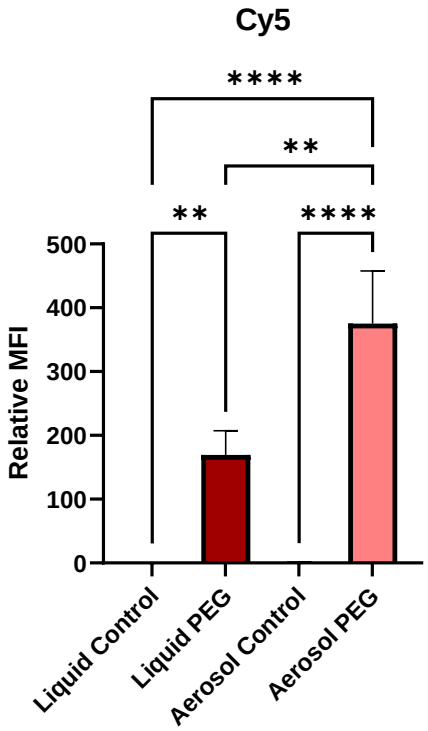

Figure 11: Relative MFI of Cy5 labeled PEGDA nanoparticles uptaken by A549 cells using liquid and aerosol dosing methods. Relative MFI measurements are displayed as the average and standard deviation of three experimental replicates. *$p < 0.05$, **$p < 0.01$, ***$p < 0.001$, ****$p < 0.0001$, ns = not significant using Tukey's multiple comparisons tests as part of a one-way ANOVA (n = 3).

As seen in **Figure 11** above, there was significant nanoparticle uptake using both liquid and aerosol dosing methods. Statistical significance was determined using Tukey's multiple comparisons tests as part of a one-way ANOVA. While both dosing

methods showed significant nanoparticle uptake, the aerosol dosing method produced a greater relative MFI compared to the liquid dosing method. This result could be attributed to the higher nanoparticle concentration used for the aerosol dosing method and an inconsistent nebulizer yield. Additionally, aerosol dosing can cause cell apoptosis due to the cells having to be out of liquid for a period of time and the nanoparticles dosed were suspended in PBS, rather than media. With greater cell apoptosis, the aerosol dosing group had a higher percentage of live cells that uptake nanoparticles than the liquid dosing group, which had a greater amount of live cells total, and in turn had a smaller percentage of cells that uptake nanoparticles, causing its relative MFI to be lower than the aerosol dosed group.

To assess cell viability after liquid and aerosol dosing of PEGDA nanoparticles, cells were stained with Zombie Yellow, which marks cells that are undergoing pre apoptosis. Zombie Yellow dye is an amine-reactive dye that is non-permeant for live cells but permeant for dead cells. The dye detects amines on the surface of all cells; however, since dying cells have compromised membranes, it can access and bind to the numerous intracellular amines of dead cells. Therefore, Zombie Yellow intensely stains dead cells, while live cells only receive a low level of surface staining. Flow cytometry was used to quantify cell viability after dosing by measuring Zombie Yellow fluorescence, in which the results are displayed in **Figure 12** below.

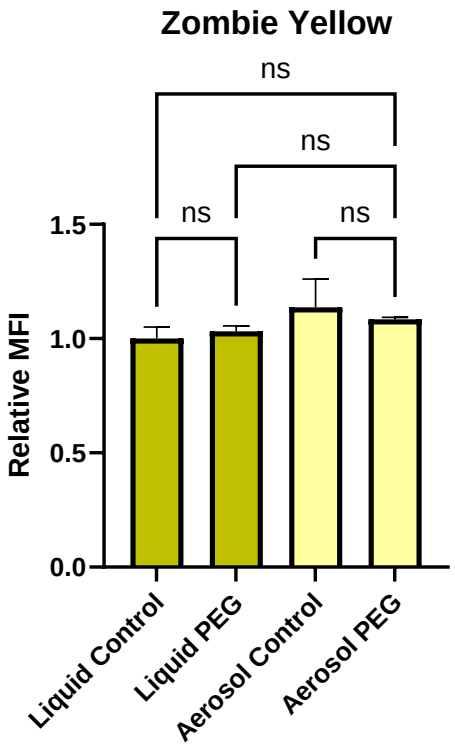

Figure 12: Relative MFI of A549 cells stained with Zombie Yellow after liquid and aerosol dosing of PEGDA nanoparticles. Relative MFI measurements are displayed as the average and standard deviation of three experimental replicates. *$p < 0.05$, **$p < 0.01$, ***$p < 0.001$, ****$p < 0.0001$, ns = not significant using Tukey's multiple comparisons tests as part of a one-way ANOVA (n = 3).

As seen in **Figure 12** above, there was little cell death associated with both dosing methods of PEGDA nanoparticles. Statistical significance for each treatment group was determined using Tukey's multiple comparisons tests as part of a one-way ANOVA. Notably, the aerosol dosing method did not cause significant cell apoptosis compared to the liquid dosing method, as displayed by the liquid and aerosol control groups. Additionally, there was no increase in cell apoptosis when dosed with liquid PEGDA nanoparticles compared to the liquid control group, indicating that the

PEGDA nanoparticles do not cause cell apoptosis. This result is consistent for cells dosed with aerosol PEGDA nanoparticles compared to the aerosol control group.

4.2 Polyplex Nanoparticle Dosing

After successful uptake of PEGDA nanoparticles by A549 cells using both liquid and aerosol dosing methods, polyplexes were dosed to A549 cells using both dosing methods for nucleic acid delivery. Successful delivery of these nanoparticles was determined by cell transfection, which was quantified by the production of GFP, as well as cell viability after dosing. In order to characterize the effects of liquid and aerosol dosing on polyplex cell transfection by A549 cells, there were four treatment groups: the liquid control group was dosed with incomplete liquid media without polyplexes, the liquid polyplex group was dosed with incomplete liquid media containing polyplexes at a concentration of 20 µg/mL, the aerosol control group was dosed with aerosolized incomplete media without polyplexes, and the aerosol polyplex group was dosed with aerosolized incomplete media containing polyplexes at a concentration of 20 µg/mL.

4.2.1 Polyplex Characterization

Polyplexes were generated and characterized to determine sample concentration, hydrodynamic diameter, and PDI. The sample was found to have an average hydrodynamic diameter of 103.1 ± 2.124 nm and an average PDI of 0.1447 ± 0.011. This particle size is consistent with synthesis values reported in literature.[12] The measured PDI indicates that the polyplexes were narrowly monodisperse.

4.2.2 Polyplex Cell Transfection Microscopy

All A549 cell treatment groups were imaged 24 and 48 hours after polyplex administration using the Zeiss Axio Observer 7 and the Biotek Cytation 5 Imager, respectively, in order to visualize cell transfection and cell viability after polyplex dosing. These images are depicted in **Figures 13 and 14** below.

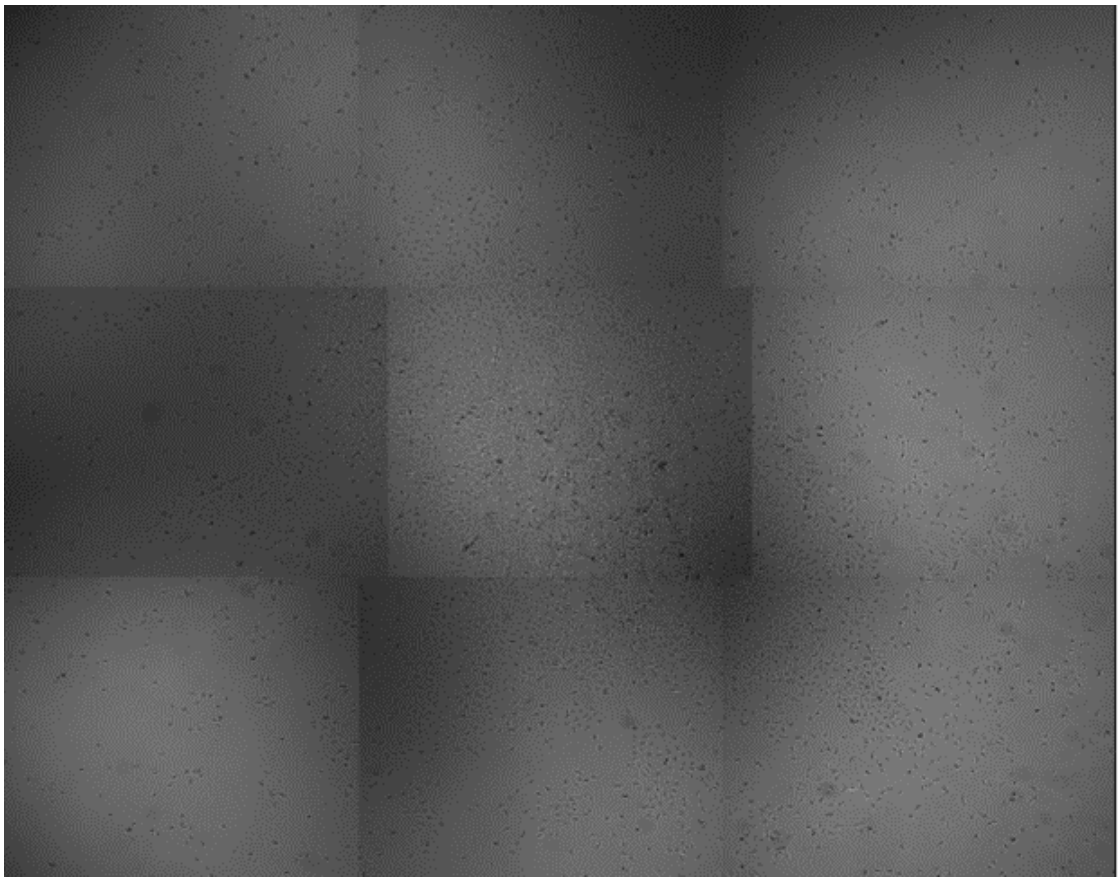

Figure 13: Micrograph of A549 cells 24 hours after aerosol polyplex dosing.

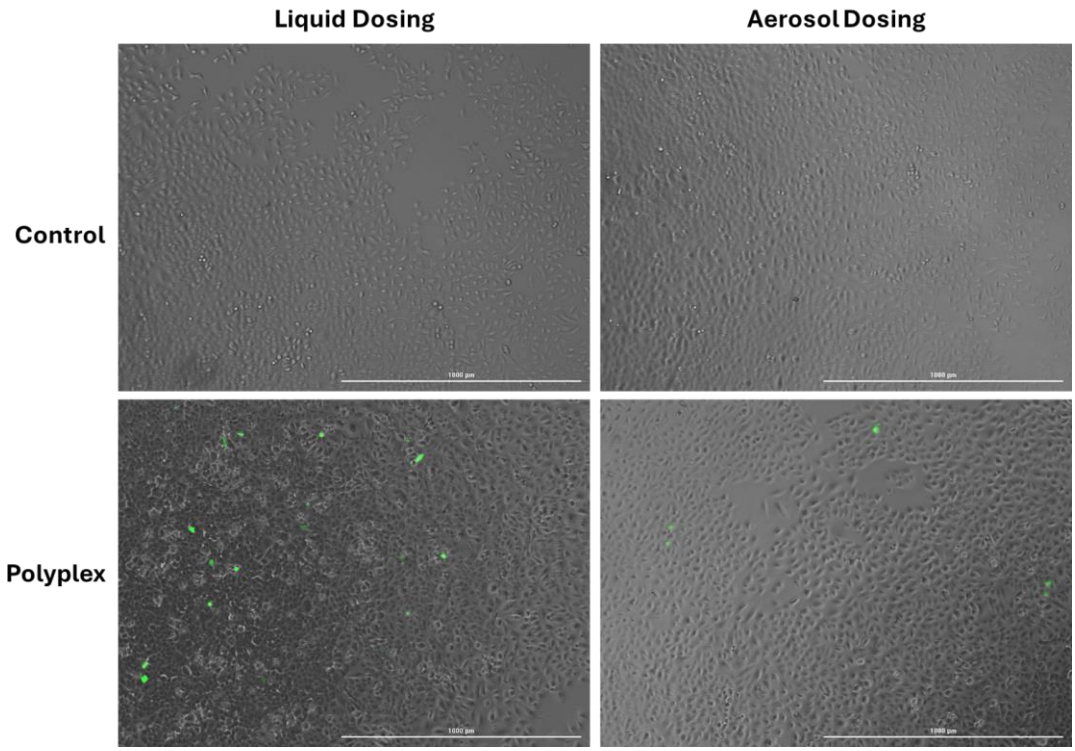

Figure 14: Micrographs of A549 cells 48 hours after liquid and aerosol polyplex dosing.

As seen in **Figures 13 and 14** above, GFP was produced by cells dosed with polyplexes using both liquid and aerosol dosing methods. GFP was not produced in either of the control groups, signifying that the production of GFP was a result of cellular transfection by polyplexes. These results visually indicate that liquid and aerosol dosing of polyplexes cause transfection in A549 cells. However, as seen in the micrographs above, it appears the liquid dosing method produced a greater amount of GFP than the aerosol dosing method, despite relatively equivalent DNA dosing for both dosing methods. This could be a result of low nebulizer yields or deformation of the polyplexes when passed through the vibrating mesh nebulizer. Further experimental analysis is needed to confirm this result, such as DLS. The

hydrodynamic diameter of the polyplexes could be measured using DLS before and after nebulization, in which an increase in hydrodynamic diameter would indicate the polyplexes cannot be stably nebulized. Furthermore, the micrographs of the polyplex administered groups in Figure 13 depict increased cell death compared to the control groups, especially in the aerosol polyplex treated group. This increase in cell death is to be expected due to the high cytotoxicity of polyplexes. As described previously, polyplexes are synthesized using PEI, a cationic, positively charged, polymer allowing it to form a complex with negatively charged DNA. While positively charged particles can enter cells more easily, increasing cell transfection, they are also highly cytotoxic, limiting their efficacy. Therefore, for increased cell viability, the N/P ratio of the polyplexes should be optimized for effective cell transfection without causing significant cell death.

4.2.3 Polyplex Cell Transfection Flow Cytometry

In order to quantify cell transfection of A549 cells after liquid and aerosol dosing of polyplexes, flow cytometry was performed 48 hours after initial dosing to measure GFP fluorescence, in which the results are displayed in **Figure 15** below.

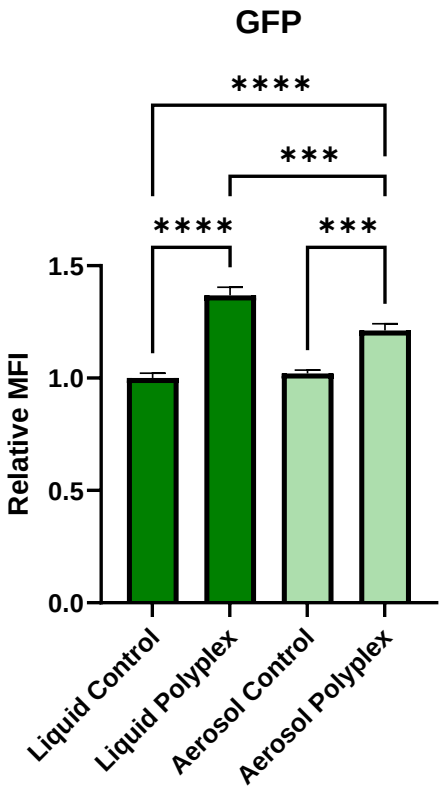

Figure 15: Relative MFI of GFP produced by A549 cells 48 hours after liquid and aerosol dosing of polyplexes. Relative MFI measurements are displayed as the average and standard deviation of three experimental replicates. *p < 0.05, **p < 0.01, ***p < 0.001, ****p < 0.0001, ns = not significant using Tukey's multiple comparisons tests as part of a one-way ANOVA (n = 3).

As seen in **Figure 15** above, there was significant GFP production from liquid and aerosol dosing of polyplexes to A549 cells, indicating successful cell transfection. Statistical significance was determined using Tukey's multiple comparisons tests as part of a one-way ANOVA. Additionally, the results depicted by flow cytometry agree with and quantify the visualized results of the micrographs in **Figures 13 and 14**

above; liquid dosing of polyplexes resulted in greater cell transfection than aerosol dosing.

To assess cell viability after liquid and aerosol dosing of polyplexes, cells were stained with Zombie Yellow 48 hours after initial dosing to mark cells undergoing pre apoptosis. Flow cytometry was used to quantify cell viability after dosing by measuring Zombie Yellow fluorescence, in which the results are displayed in **Figure 16** below.

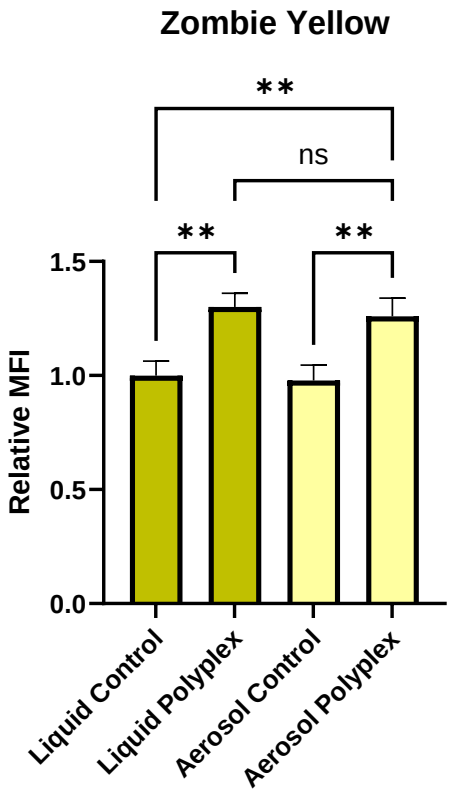

Figure 16: Relative MFI of A549 cells stained with Zombie Yellow 48 hours after liquid and aerosol dosing of polyplexes. Relative MFI measurements are displayed as the average and standard deviation of three experimental replicates. *$p < 0.05$, **$p < 0.01$, ***$p < 0.001$, ****$p < 0.0001$, ns = not significant using Tukey's multiple comparisons tests as part of a one-way ANOVA (n = 3).

As seen in **Figure 16** above, there was significant cell death after liquid and aerosol dosing of polyplexes. Statistical significance was determined using Tukey's multiple comparisons tests as part of a one-way ANOVA. These results confirm the increased number of dead cells seen in the polyplex treatment groups displayed by the micrographs in **Figures 13 and 14** above. There was also no significant increase in cell apoptosis in the aerosol control group compared to the liquid control group, which further supports that the polyplexes are causing cell apoptosis.

Chapter 5

CONCLUSIONS AND FUTURE WORK

5.1 Conclusions

This work begins to characterize a formulation pathway for the application of a nebulized nanoparticle-loaded aerosol vaccine delivery system that displays potential on the cellular and macroscopic level. While this work only provides a superficial analysis of this delivery system, notable conclusions can be drawn from these results that can be applied to nucleic acid delivery, as well as aerosol drug delivery as a whole.

5.1.1 Physical Effects of Nanoparticle Loading on Nebulized Aerosols

In this work, the physical effects of nanoparticle loading into nebulized aerosols were explored using both laser diffraction and microscopic measurement methods. Specifically, the effects of nebulizer loading volume and nanoparticle loading concentration on aerosol size were analyzed. From the optical particle sizing results, it can be concluded that the nebulizer loading volume has no effect on the size of the nebulized aerosol. Additionally, it was found that the size of the aerosol increases with increasing nanoparticle concentration. This is significant for many aerosol drug delivery applications since the size of the aerosol directly correlates with lung deposition. Aerosol particles that are too large will deposit in the mouth and throat, while aerosols that are too small have a high likelihood of being exhaled. For effective lower respiratory tract impaction, inhaled aerosols should be between 1 and 5

µm.[7] The optical particle sizing results from this work show that with high nanoparticle loading concentrations, the VMD of nebulized aerosols can exceed 7 µm, indicating that these aerosol droplets would impact in the mouth and throat, lowering the efficacy of an aerosol therapeutic. Therefore, nanoparticle loading in nebulized aerosols should be optimized for desired aerosol deposition.

5.1.2 Nanoparticle Mediated Nucleic Acid Delivery

In this work, the effects of liquid and aerosol nanoparticle delivery methods on nanoparticle-mediated nucleic acid delivery were assessed. These results were determined through the quantification of PEGDA nanoparticle uptake, as well as polyplex induced cell transfection, by A549 cells using both liquid and aerosol delivery methods. Successful nanoparticle uptake and cell transfection by polyplexes with liquid and aerosol delivery were measured using flow cytometry. While the liquid dosing method was shown to be more effective, the results from this work provide a proof of concept for nanoparticle-mediated nucleic acid delivery using nebulized aerosols. Notably, this work indicates the stability of polyplexes to be aerosolized, providing a foundation for a more effective pulmonary nucleic acid delivery system. However, while aerosol drug delivery provides many benefits for pulmonary applications as opposed to systemic drug delivery methods, the nanoparticle-loaded aerosol delivery platform characterized in this work would need to be optimized to begin to see the aerosol delivery efficiencies exceed those of existing liquid dosing methods.

5.2 Future Work

The results of this work indicate great potential for future work. Given the effects of nanoparticle loading concentration alone on the size of nebulized aerosols, the effect of other nanoparticle characteristics on aerosol size could be assessed for effective lung deposition. Additionally, the proof-of-concept nanoparticle mediated nucleic acid delivery system characterized in this work could be optimized for higher cell transfection efficiencies and cell viability, increasing the potential for viable pulmonary delivery platforms.

5.2.1 Physical Effects of Nanoparticle Loading on Nebulized Aerosols

As seen by the results in this work, aerosol size increases with increasing nanoparticle concentration. Given the correlation and effects of aerosol size on lung deposition, the characterization of other nanoparticle characteristics could be indicative of effective targeted lung deposition of nebulized aerosols for pulmonary drug delivery applications. Specifically, the effects of nanoparticle loading size and charge on the size of nebulized aerosols could be assessed for effective lung deposition and mucosal transport. In this current work, the effects of four concentrations of 1 micron particles on nebulized aerosols were measured. However, nucleic acid nanoparticle carriers are typically much smaller, such as polyplexes, which are approximately 100 nm. Therefore, studies using nanoparticles of sizes exemplary of potential nucleic acid nanoparticle carriers should be conducted. Additionally, many nanoparticle carriers have a charge associated with them, including polyplexes, making the effect of nanoparticle charge on the size of nebulized aerosols a useful characteristic to measure. In future work, a DOE approach could be used to assess the effect of nanoparticle concentration, size, and charge on nebulized

aerosols in order to create aerosol formulations with tunable nanoparticle loadings and aerosol sizes for enhanced lung deposition and mucosal penetration.

5.2.2 Nanoparticle Mediated Nucleic Acid Delivery

While this work provides a proof of concept for aerosol delivery of nucleic acid loaded nanoparticles, much optimization is needed to make this platform viable for pulmonary applications. To begin, cell transfection efficiency using aerosol dosing was lower than that of liquid dosing, indicating the need to improve the aerosol delivery method. However, most significantly, both liquid and aerosol polyplex dosing methods showed a significant decrease in cell viability. This is likely due to the cytotoxicity of the PEI used to form the polyplexes. Therefore, methods to decrease polyplex cytotoxicity are needed. Current literature reports that polyplexes formulated with PEI and H3 tail peptides showed significantly greater cell transfection without compromising cell viability.[12] Future work could include assessing the aerosol delivery method using newly formulated polyplexes, such as those with H3 tail peptides. Furthermore, future work could also include assessing the efficacy of other types of nucleic acid nanoparticle carriers. For example, lipid nanoparticles (LNPs) have shown much promise for mRNA delivery therapeutics; therefore, the efficacy and stability of LNPs to be aerosolized could be a promising direction for future work for pulmonary nucleic acid and gene delivery applications.

5.3 Impact

The work presented in this thesis has potential to have significant impacts on particulate aerosol delivery systems, as well as nucleic acid delivery applications. As of currently, this work is the first time that nanoparticle concentration has been shown

to have an effect on aerosol droplet size, which has significant implications for nebulization of any particulate based nebulized formulation. Therefore, this finding could be continued and extended to different particle sizes, concentrations, and charges in order to create tunable aerosols for more precise lung deposition targeting, which could improve lung mucosal transport and therapeutic immunogenicity. Furthermore, the ability for aerosolized polyplexes to transfect cells indicates their stability when nebulized. This also has significant impacts on gene delivery applications, suggesting that with future work, gene delivery vectors are stable enough to be nebulized in order to treat pulmonary diseases.

REFERENCES

(1) Prevalence and attributable health burden of chronic respiratory diseases, 1990-2017: a systematic analysis for the Global Burden of Disease Study 2017. *Lancet Respir Med* **2020**, *8* (6), 585-596. DOI: 10.1016/s2213-2600(20)30105-3 From NLM.
(2) Restrepo, M. I.; Keyt, H.; Reyes, L. F. Aerosolized Antibiotics. *Respiratory Care* **2015**, *60* (6), 762. DOI: 10.4187/respcare.04208.
(3) Muralidharan, P.; Malapit, M.; Mallory, E.; Hayes, D.; Mansour, H. M. Inhalable nanoparticulate powders for respiratory delivery. *Nanomedicine: Nanotechnology, Biology and Medicine* **2015**, *11* (5), 1189-1199. DOI: https://doi.org/10.1016/j.nano.2015.01.007.
(4) Heida, R.; Hinrichs, W. L. J.; Frijlink, H. W. Inhaled vaccine delivery in the combat against respiratory viruses: a 2021 overview of recent developments and implications for COVID-19. *Expert Review of Vaccines* **2022**, *21* (7), 957-974. DOI: 10.1080/14760584.2021.1903878.
(5) Sudduth, E. R.; Trautmann-Rodriguez, M.; Gill, N.; Bomb, K.; Fromen, C. A. Aerosol pulmonary immune engineering. *Advanced Drug Delivery Reviews* **2023**, *199*, 114831. DOI: https://doi.org/10.1016/j.addr.2023.114831.
(6) Darquenne, C. Aerosol deposition in health and disease. *J Aerosol Med Pulm Drug Deliv* **2012**, *25* (3), 140-147. DOI: 10.1089/jamp.2011.0916 From NLM.
(7) Jabbal, S.; Poli, G.; Lipworth, B. Does size really matter?: Relationship of particle size to lung deposition and exhaled fraction. *Journal of Allergy and Clinical Immunology* **2017**, *139* (6), 2013-2014.e2011. DOI: 10.1016/j.jaci.2016.11.036 (acccessed 2024/05/12).
(8) Mitchell, J. P.; Nagel, M. W.; Nichols, S.; Nerbrink, O. Laser Diffractometry as a Technique for the Rapid Assessment of Aerosol Particle Size from Inhalers. *Journal of Aerosol Medicine* **2006**, *19* (4), 409-433. DOI: 10.1089/jam.2006.19.409 (acccessed 2024/05/12).
(9) Zeiger, A. S.; Hinton, B.; Van Vliet, K. J. Why the dish makes a difference: quantitative comparison of polystyrene culture surfaces. *Acta Biomater* **2013**, *9* (7), 7354-7361. DOI: 10.1016/j.actbio.2013.02.035 From NLM.
(10) Li, Y.; Pham, J. Q.; Johnston, K. P.; Green, P. F. Contact Angle of Water on Polystyrene Thin Films: Effects of CO2 Environment and Film Thickness. *Langmuir* **2007**, *23* (19), 9785-9793. DOI: 10.1021/la0636311.
(11) Jarai, B. M.; Fromen, C. A. Nanoparticle Internalization Promotes the Survival of Primary Macrophages. *Adv Nanobiomed Res* **2022**, *2* (5). DOI: 10.1002/anbr.202100127 From NLM.

(12) Reilly, M. J.; Larsen, J. D.; Sullivan, M. O. Histone H3 Tail Peptides and Poly(ethylenimine) Have Synergistic Effects for Gene Delivery. *Molecular Pharmaceutics* **2012**, *9* (5), 1031-1040. DOI: 10.1021/mp200372s.
(13) Millili, P. G.; Yin, D. H.; Fan, H.; Naik, U. P.; Sullivan, M. O. Formulation of a Peptide Nucleic Acid Based Nucleic Acid Delivery Construct. *Bioconjugate Chemistry* **2010**, *21* (3), 445-455. DOI: 10.1021/bc900328j.